Journal of Alloys and Compounds 727 (2017) 168–176

Contents lists available at ScienceDirect

Journal of Alloys and Compounds

journal homepage: http://www.elsevier.com/locate/jalcom

The effect of cobalt-doping on microstructure and dielectric properties of $CaCu_3Ti_4O_{12}$ ceramics

Zahra Kafi [a], Ahmad Kompany [a, b, *], Hadi Arabi [c], Ali Khorsand Zak [d]

[a] Materials and Electroceramics Laboratory, Department of Physics, Faculty of Science, Ferdowsi University of Mashhad, Mashhad, Iran
[b] Nano Research Center, Ferdowsi University of Mashhad, Mashhad, Iran
[c] Renewable Energies, Magnetism and Nanotechnology Research Laboratory, Department of Physics, Faculty of Science, Ferdowsi University of Mashhad, Mashhad, Iran
[d] Nanotechnology Laboratory, Esfarayen University of Technology, North Khorasan, Iran

ARTICLE INFO

Article history:
Received 16 February 2017
Received in revised form
20 June 2017
Accepted 23 July 2017
Available online 26 July 2017

Keywords:
$CaCu_{3-x}Co_xTi_4O_{12}$
Semi-wet method
Dielectric properties
Grain boundaries
Cu-rich phase

ABSTRACT

Ceramics of $CaCu_{3-x}Co_xTi_4O_{12}$ (CCCTO, x = 0, 0.2, 0.4 and 0.6), with cubic lattice structure, were fabricated using a semi-wet method. The dielectric properties of the prepared samples were studied at 1 kHz frequency in the temperature range of 300–600 K, as well as in the frequency range of 50 Hz–200 kHz at room temperature. The results showed that the dielectric constants of the as-prepared samples in the frequency range of 50 Hz–200 kHz, at room temperature, are reasonably high ($1.7 \times 10^4 \leq \varepsilon \leq 6 \times 10^4$). It was also found out that the dielectric loss ($\tan\delta$) of the prepared samples decreased by increasing the cobalt concentration at low and middle frequencies. The dielectric loss decreased from 0.87 for an undoped sample $CaCu_3Ti_4O_{12}$ (CCTO), to 0.15 for a doped sample (CCCTO) with x = 0.6, at 50 Hz frequency. However, the dielectric constant (ε) values for the samples doped with cobalt were found to be higher than that of for the undoped sample. Moreover, the XRD patterns as well as the SEM images and EDX results revealed that the Cu-rich phase (CuO) decreased at the CCTO grain boundaries, while at the same time Co_2TiO_4 and $CaTiO_3$ phases with good dielectric insulating behavior having been formed at the boundaries. This causes the increase of the resistance at the grain boundaries leading to lower leakage current which in turn results in a decrease of the dielectric loss. These results were confirmed by using the impedance spectroscopy analysis. Our results indicate that the cobalt doped CCTO ceramics can be suggested as good candidates to be used in fabricating microelectronic and memory devices with high dielectric constant and low dielectric loss.

1. Introduction

In the last two decades, calcium copper titanate (CCTO), due to its giant dielectric constant (>10^4) as well as good thermal and frequency stability, in the temperature range of 100–600 K and frequencies up to 10^6 Hz, has attracted much attention in a variety of applications such as fabricating microelectronic and memory devices [1–3]. However, the thermal independence of the CCTO dielectric constant has not been seen in ferroelectric materials, which makes the ferroelectric materials unsuitable to be used for various applications [2]. Theoretical studies have shown that CCTO can have a dielectric constant of about 40–50 [2,4,5], while the obtained experimental values are extremely higher. In other words, this high dielectric constant has roots in the extrinsic nature of CCTO ceramics. It has been suggested that this behavior corresponds to the microstructure of these ceramics, in which in their structure semiconducting grains are surrounded by CuO phase [1,6]. It has also been reported that the presence of an internal barrier layer capacitance (IBLC), at T > 100 K, is responsible for the giant dielectric constant in CCTO ceramics [7,8]. This phenomenon is associated with Maxwell-Wagner mechanism, which is the main characteristic of the electric materials having non-homogenous structures [9]. In addition, the impedance spectroscopy results of CCTO ceramics have revealed that there is a big difference between the resistance of the grains and the grain boundaries. This big difference in the resistance results in the formation of a large internal barrier and therefore increases the CCTO dielectric constant [5]. Another important parameter regarding the dielectric properties of

* Corresponding author. Materials and Electroceramics Laboratory, Department of Physics, Faculty of Science, Ferdowsi University of Mashhad, Mashhad, Iran.
E-mail address: kompany@um.ac.ir (A. Kompany).

http://dx.doi.org/10.1016/j.jallcom.2017.07.236
0925-8388/

CCTO is the dielectric loss (tanδ), which is directly related to the conductivity of the grain boundaries [10–12]. The impedance spectroscopy analysis has confirmed the relation between the dielectric loss (tanδ) and the conductivity at the grain boundaries, in CCTO ceramics. The increase of the conductivity at the grain boundaries causes the increase of the leakage current which in turn results in a higher dielectric loss [13]. Many attempts have been made to reduce the dielectric loss in CCTO ceramics, since the high tanδ makes it less appropriate to be used in microelectronic devices [14]. The greatest tendencies for decreasing tanδ have been found to be along with the reduction in the dielectric constant [13,15–21]. In CCTO ceramics, the content of Cu has a significant influence on its dielectric properties [22]. Chun-Hong Mu et al. [13] have doped Sr^{2+} at Cu^{2+} site in the CCTO ceramic. Their results showed changes in the grain boundaries structure caused a reduction in the dielectric loss as well as a decrease in the dielectric constant to less than 10^4. Yueyue Yan et al. [15] have reported that adding $CaTiO_3$ into CCTO ceramic and its congregation at the boundaries reduced the tanδ along with the decrease in the dielectric constant to the values less than 5000. According to these studies, it seems to be possible to decrease the dielectric loss (tanδ) by controlling the structure and chemistry of the grain boundary regions in CCTO ceramics. Our main objective has been to reduce the dielectric loss (together with the increase of the dielectric constant) in CCCTO ceramics by decreasing the leakage current, due to the reduction in the grain boundaries conductivity. This has been done by reducing the CuO phase, with semiconducting behavior [23], and the formation of $CaTiO_3$ and Co_2TiO_4 phases with good dielectric insulating properties [24–26] in the grain boundaries, through substitution of Co^{2+} in Cu^{2+} site in CCTO ceramic. To find out the effect of substituting Cu^{2+} by Co^2 on the dielectric constant and loss values, we have investigated the microstructure of the grain boundaries in detail.

2. Experimental

2.1. Materials and method

$Ca(NO_3)_2{\cdot}4H_2O$ (purity 98%, Merck), $Cu(NO_3)_2{\cdot}3H_2O$ (purity 99%, Merck), $Co(NO_3)_2{\cdot}6H_2O$ (purity 97%, Merck), TiO_2 (purity 99.5%, Merck) and citric acid (purity 99.5%, Merck) were used as the starting materials and distilled water as the solvent. Proper amounts of these materials were selected based on the $CaCu_{3-x}Co_xTi_4O_{12}$ (CCCTO) (x = 0, 0.2, 0.4 and 0.6) formula. First, a solution of the nitrates was prepared and, at the same time, the suspension of TiO_2 powder and citric acid was made using minimum amounts of water. The amount of citric acid was chosen equivalent to the metal cations and the nitrates solution was added to the suspension. The final solution was kept at 70–80 °C temperature, under vigorous stirring, and then dried in an oven at 90 °C for 12 h, until a blue gel was obtained. The gel was calcined at 850 °C for 8 h in a muffle furnace. After grinding the calcined powder, it was pressed into pellets with 10 mm in diameter and 2 mm in thickness, under 250 MPa using a hydraulic press. Finally, the prepared disks were sintered in air at 1050 °C for 15 h.

2.2. Characterization methods

The X-ray diffractometer (XRD- D8 ADVANCED-BRUKER) with Cu $K\alpha_1$ radiation (λ = 1.5406 Å) was employed to investigate the crystal structure of the prepared samples. Scanning electron microscopy (SEM- LEO 1450VP) equipped with energy dispersive X-ray analyzer (EDX- OXFORD) was used to study the surface morphology and the local elemental analysis of the grains and grain boundaries. To measure the dielectric properties of the prepared ceramics, both faces of the disks were coated with silver paste and cured in the hot air oven at 220 °C for 2 h. The LCR meter (LCR 811 0G INSTEK) was used to measure the dielectric constant and the tanδ in the frequency range of 50 Hz–200 kHz at room temperature as well as at 1 kHz in the temperature range of 300–600 K.

3. Results and discussion

3.1. X-ray diffraction analysis

Fig. 1(a and b) illustrates the X-ray diffraction patterns of the $CaCu_{3-x}Co_xTi_4O_{12}$ (CCCTO) ceramics (x = 0, 0.2, 0.4 and 0.6) sintered at 1050 °C for 15 h. As the patterns show, the CCTO cubic crystal phases with the space group $Im\bar{3}$ have been formed in accordance with JCPDS card No. 21-0140, in all prepared samples. It is obvious that the peaks of CuO phase can only be observed in the undoped sample. By adding cobalt into CCTO, the peaks related to $CaTiO_3$ and Co_2TiO_4 structures appear. The intensities of $CaTiO_3$ and Co_2TiO_4 peaks are enhanced by increasing the cobalt concentration.

3.2. Microstructural studies

The back scattered electron SEM images and their corresponding grain size histograms are presented in Fig. 2, which illustrates the surface morphology of the prepared ceramics. These figures indicate that with the increase in Co^{2+} concentration from x = 0 up to x = 0.4, the size of the grains first becomes larger and thereafter decreases for x = 0.6 as shown in Fig. 2(b, c and d). Furthermore, the exfoliated sheets with lighter color in the images are appeared between the grains mainly due to the presence of Cu-rich phase (CuO) [27,28]. Also this is proved by the EDX results. It is believed that the densification of the ceramics is somehow caused by the liquid phase that is formed during the sintering step [16,29]. By comparing the SEM images of the pure and cobalt doped samples, it can be concluded that the amount of the Cu-rich phase has been reduced remarkably in the doped samples along with the formation of Co_2TiO_4 and $CaTiO_3$ at the grain boundaries. These results are also confirmed by EDX, as shown in Fig. 3 (lower shapes are for the grains and upper ones for the grain boundaries, shown with yellow arrows) as well as the XRD analysis (Fig. 1(b)). The average grain size values of the samples with x = 0, 0.2, 0.4 and 0.6 are found about 48, 108, 107 and 75 μm, respectively. First, by increasing the cobalt concentration the CuO secondary phase (light color in Fig. 2(b and c)) decreases at the grain boundaries, which results in speeding up the grain growth. So, the grains become larger for the samples with x = 0.2 and 0.4. When the amount of cobalt concentration increases further and passes the critical limit (x = 0.6), the amounts of $CaTiO_3$ and Co_2TiO_4 secondary phases, which have already appeared at the grain boundaries in the samples with x = 0.2 and x = 0.4 increase, causing the grain growth limitation. XRD results, Fig. 1(b), confirmed the decrease of the CuO as well as increasing the amounts of $CaTiO_3$ and Co_2TiO_4 phases. This phenomenon is called the pinning effect, which says that the critical grain size depends on the definite volume fraction of the secondary phases in the grain boundaries. So that, for the amounts of more than this definite volume fraction, further growth of the grains is inhibited and pinned [30–33]. This phenomenon seems to occur for the sample with x = 0.6.

The giant grains observed in our samples have also been reported by some other researchers [13,34,35]. As mentioned earlier, other researchers have reported that the presence of the Cu-rich phase at the grain boundaries is an important factor which affects the tanδ value. The grain boundaries were investigated further by using SEM and EDX. Fig. 3 is the back scattered electron SEM images of the grains and grain boundaries of the ceramic samples along

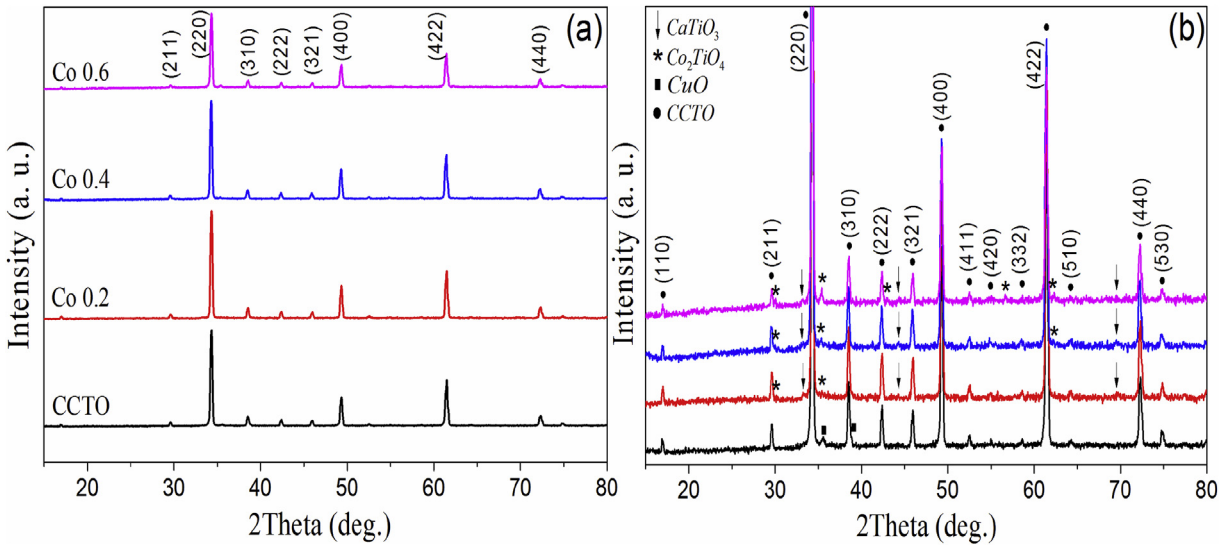

Fig. 1. X-ray diffraction patterns of (a) $CaCu_{3-x}Co_xTi_4O_{12}$ ceramics sintered at 1050 °C for 15 h and (b) the corresponding expanded patterns. The peaks are indexed for cubic structure of CCTO.

with their EDX. As it can be seen in Fig. 3(a), for the pure sample the thickness of the grain boundaries and the amount of the Cu-rich phase are remarkably large, compared to the doped samples (Fig. 3(b–d)). These figures show that by increasing the amount of Co^{2+}, from x = 0.2 to x = 0.6, the thickness of the grain boundaries and also the amount of the Cu-rich phase have been reduced, and at the same time, Co_2TiO_4 and $CaTiO_3$ phases have been formed at the grain boundaries. These results are further confirmed by the XRD analysis (Fig. 1(b)). The EDX of the grains (Fig. 3, lower shapes) indicates that by increasing the amount of Co^{2+} dopant, only the amount of Co^{2+} in the grains has increased, while at the grain boundaries (Fig. 3, upper shapes) the Cu-rich phase decreased along with the formation of Co_2TiO_4 and $CaTiO_3$ phases.

3.3. Bulk density determination

The bulk densities of the prepared ceramics were determined 4.85, 4.65, 4.61 and 4.52 g/cm^3 for the samples with x = 0, 0.2, 0.4 and 0.6, respectively using Archimedes method. The density of the ceramic pellets slightly decreased with the increase of Co^{2+} concentration, since the atomic weight of cobalt (58.93 g) is smaller than that of copper (63.54 g). Moreover, as mentioned earlier, in the sintering process the second liquid phase at the grain boundaries results in the densification of the pellets. However, since the thickness of the secondary phase has remarkably decreased in doped samples, the density of the pellets was reduced by increasing the cobalt dopant concentration, in agreement with some other reports [16,29], which is confirmed by the SEM images (Fig. 2).

3.4. Dielectric property studies

The effect of temperature on the dielectric constant and tanδ of the prepared samples was investigated at 1 kHz in the temperature range of 300–600 K, Fig. 4(a and b). The dielectric constants obtained for all the samples were greater than 10^4, in the whole range of temperature. As it can be seen in Fig. 4(a), from room temperature to about 400 K no remarkable changes can be observed in the dielectric constant of the samples. However, at temperatures close to room temperature, the dielectric constants of the doped samples are greater than that of the undoped sample, while the dielectric losses are less. This is observed more clearly in the insets of Fig. 4(a and b). At temperatures above 450 K, the dielectric constant of the samples enhances with the increase of the temperature, which is highly noticeable for the samples with x = 0.4 and x = 0.6. The big differences in the dielectric values at high and low temperatures can be related to the movement difference of the dipoles at high and low temperatures. These remarkable increase in the dielectric constant at high temperatures along with the increase of loss is due to the high-temperature dielectric relaxation of CCTO ceramics, as has been reported previously [36,37].

In fact in an undoped sample, $CaTiO_3$ and Co_2TiO_4 compounds with high polarization properties [24–26] do not exist, but as shown in Fig. 1 (b) CuO phase with semiconducting behavior [23] is detected. So, by increasing the temperature above 450 K, the conductivity in the grain boundaries increases which is probably due to the presence of CuO, with semiconducting behavior, at the grain boundaries. This leads to a reduction in the grain boundary resistance (R_{gb}), causing a decrease in the difference between the semiconducting grain resistance (R_g) and the grain boundary resistance (R_{gb}). This results in less polarization at the grain boundaries, leading to the low dielectric constant. This process is a limiting factor for increasing the dielectric constant in the undoped sample compared to the doped samples at high temperatures, Fig. 4(a). Since with bigger R_{gb} more difference between R_{gb} and R_g appears, which results in stronger interfacial polarization leading to the increase in the dielectric constant [16]. Our results showed that in an undoped sample with high CuO content, the dielectric constant is lower in comparison with the samples with very low or without amount of CuO (doped samples) which is in agreement with the other report [22].

On the other hand, in our cobalt doped samples by increasing the cobalt concentration, the polar phases of $CaTiO_3$ and Co_2TiO_4 have increased as shown in Fig. 1(b). Therefore it can be said that due to the polarity and also the relaxation behavior in the present titanate compounds [26,38], the dielectric constant in the doped samples enhances by increasing the temperature (which is more remarkable for the samples with x = 0.4 and 0.6 having larger amounts of $CaTiO_3$ and Co_2TiO_4 phases), compared to the undoped sample which can be seen in Fig. 4(a).

Regarding what mentioned above; the existence of these phases decreases the conductivity at the grain boundaries in the doped ceramics (CuO amount decreases and at the same time, $CaTiO_3$ and

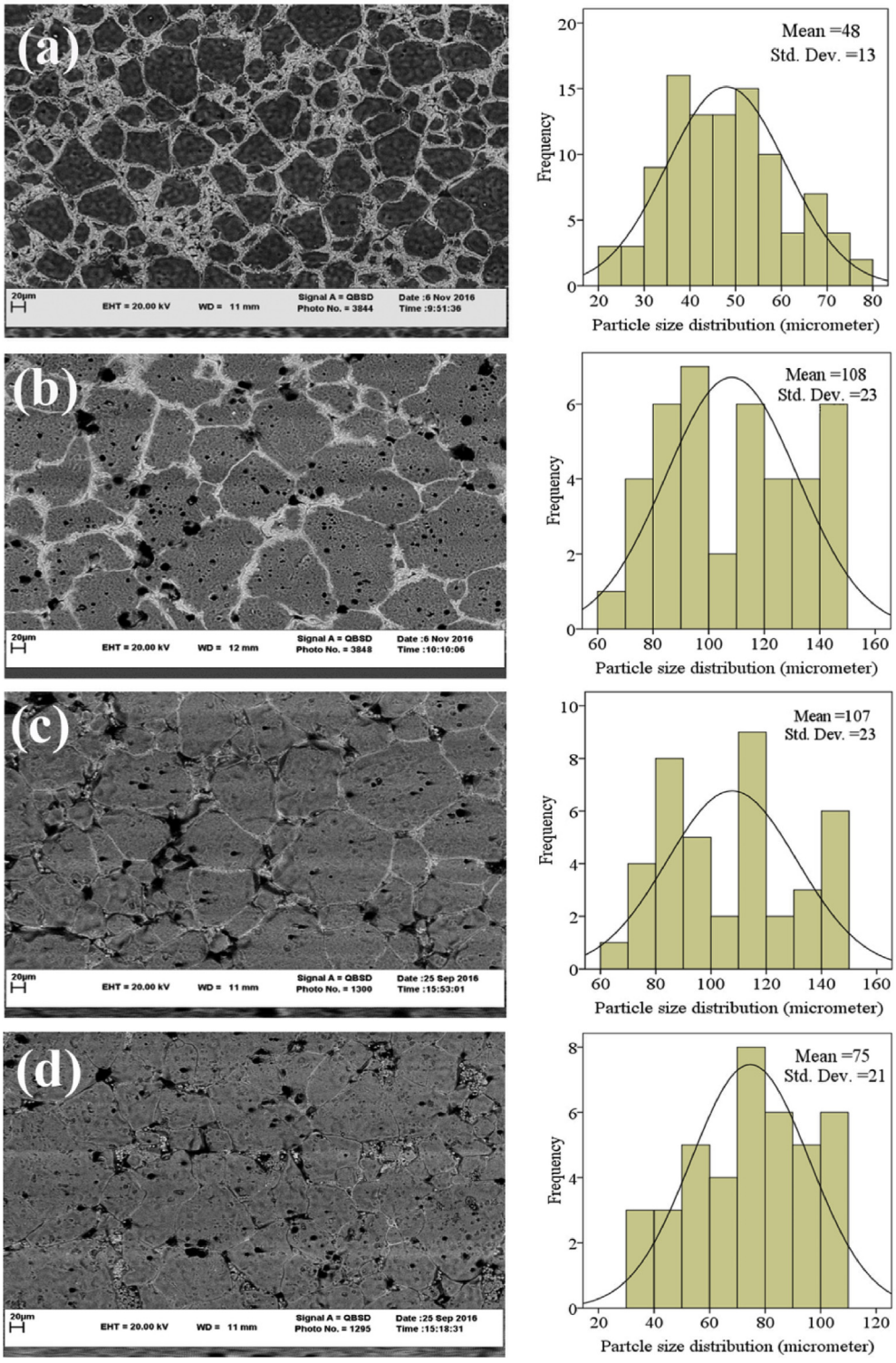

Fig. 2. Back scattered electron SEM images of $CaCu_{3-x}Co_xTi_4O_{12}$ samples (a) x = 0, (b) x = 0.2, (c) x = 0.4 and (d) x = 0.6, sintered at 1050 °C for 15 h, and the corresponding histograms.

Co_2TiO_4 phases with good dielectric insulating behavior increase). So, the dielectric loss which is directly related to the grain boundary conductivity [10–12], becomes lower in the doped samples compared to the undoped sample by increasing the temperature, as shown in Fig. 4(b).

Fig. 5(a and b) shows the dielectric constant and tanδ for the $CaCu_{3-x}Co_xTi_4O_{12}$ (x = 0, 0.2, 0.4 and 0.6) ceramics as a function of frequency, respectively. As Fig. 5(a) shows, the dielectric constant of the undoped sample at room temperature, is almost constant throughout the frequency range, which reveals that the CCTO dielectric constant is frequency independent, in agreement with previous research [39]. However, by doping Co^{+2} into the CCTO

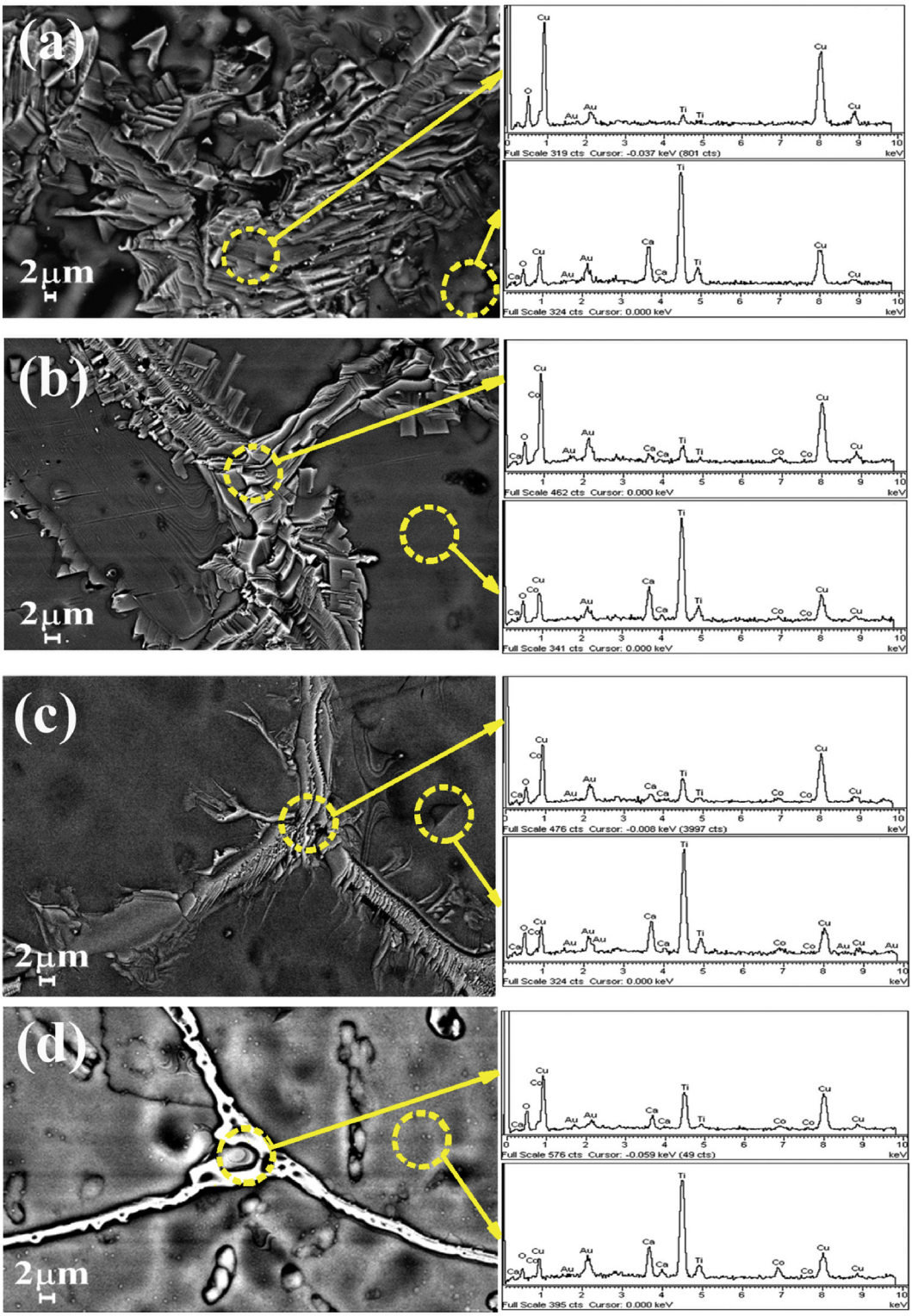

Fig. 3. Back scattered electron SEM images of $CaCu_{3-x}Co_xTi_4O_{12}$ samples (a) x = 0, (b) x = 0.2, (c) x = 0.4, (d) x = 0.6, and their EDX analysis localized on the grains and grain boundaries (lower shapes are for the grains and upper ones for the grain boundaries, shown with yellow arrows). (For interpretation of the references to colour in this figure legend, the reader is referred to the web version of this article.)

ceramic, the frequency dependence of the dielectric constant becomes remarkable, which is more significant for the frequencies less than 1 kHz. Similar results have been obtained for CCTO, in which Cu^{2+} was substituted by Fe^{3+} [40]. The values of the dielectric constant in our samples were found higher than 10^4, in all frequency range of 50 Hz–200 kHz. At 50 Hz, the dielectric constant values of the doped samples with x = 0.2, 0.4 and 0.6, were about 5.4×10^4, 5.9×10^4 and 4.5×10^4, respectively, which are

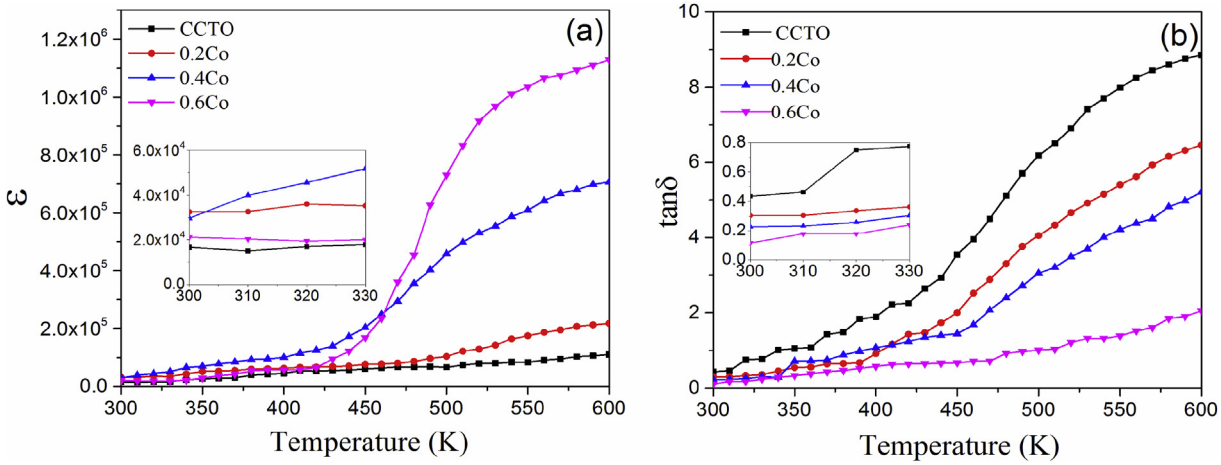

Fig. 4. Temperature dependence of (a) dielectric constant and (b) dielectric loss in $CaCu_{3-x}Co_xTi_4O_{12}$ ceramics, at 1 kHz.

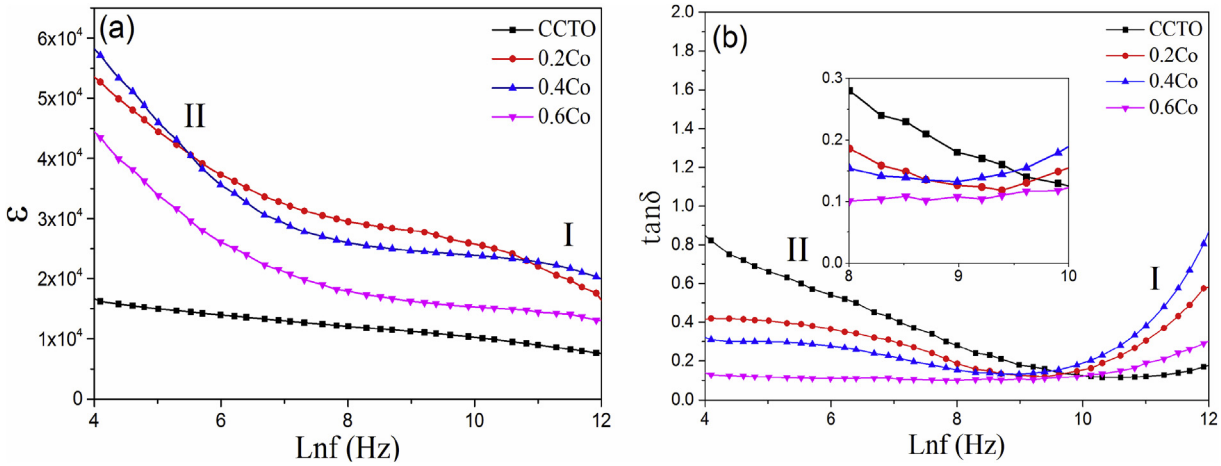

Fig. 5. Frequency dependence of (a) dielectric constant and (b) dielectric loss in $CaCu_{3-x}Co_xTi_4O_{12}$ samples, at room temperature.

remarkably larger than that of the undoped sample (1.7×10^4). As Fig. 5(a and b) illustrates, there are two dielectric relaxation processes at high and low frequencies (I and II) in both of the dielectric constant and tanδ. Relaxation I, which is observed at about 100 kHz, is related to Debye-type relaxation [41]. The second relaxation starts at about 100 Hz. It has been reported that the increase in the dielectric constant by decreasing the frequency results from interfacial and Maxwell-Wagner polarization, which occurs in the CCTO ceramics and is a very important factor for the enhancement of the dielectric constant at low frequencies [39]. Fig. 5(b) shows that for frequencies below 20 kHz, the tanδ decreases by increasing the Co^{2+} dopant concentration. This tanδ reduction is very large for the sample with x = 0.6, (tanδ = 0.15), comparing to the value for the undoped sample (tanδ = 0.87) at 50 Hz. For more clarity, the frequency dependence of tanδ is given in the inset of Fig. 5(b), in the range of 3–20 kHz. For frequencies greater than 20 kHz, the tanδ is frequency dependent, as shown in Fig. 5(b). The fast increase in tanδ at higher frequencies is due to the Debye relaxation [13]. The behavior of the dielectric constant and tanδ in the CCTO ceramic has been explained by IBLC model, in which the dielectric constant (ε) is given by the following equation [42–44]:

$$\varepsilon_r = \varepsilon_{gb}\left(d_g + d_{gb}\big/ d_{gb}\right) \quad (1)$$

where ε_{gb} is the grain boundary dielectric constant, d_g is the grain size and d_{gb} is the thickness of the grain boundary. As this equation indicates, the size of the grains plays an important role in the value of the dielectric constant. It is worth mentioning that it is not possible to obtain the exact value of the dielectric constant in the grain boundary (ε_{gb}) regions, since it is impossible to calculate the thickness and the cross-sectional area of these regions accurately [45]. According to the SEM images (Fig. 2), with the increase in Co^{2+} dopant concentration up to x = 0.4, the average size of the grains becomes larger (Fig. 2(b and c)). However, by increasing Co^{2+} concentration to x = 0.6 the average size of the grains becomes smaller (Fig. 2(d)), but is still larger than that of the undoped sample. Therefore, considering Eq. (1), one can conclude that the samples with larger grains and thinner grain boundaries, which is confirmed by the experimental results, have the higher dielectric constants [42,46].

Fig. 6 shows the Cole-Cole plots of the impedance, which can explain the tanδ behavior of the prepared $CaCu_{3-x}Co_xTi_4O_{12}$ at room temperature. The overlapped region of these curves are amplified and presented as the inset Fig. 6(a), for more clarity. By fitting the arc data, the resistance of the grains (R_g) and the grain boundaries (R_{gb}) are obtained at high and low frequencies, respectively (given in Table 1). The experimental frequency increases along the direction of the arrow in Fig. 6(b).

According to IBLC model, the tanδ at low frequencies, given by the following equation [15,43]:

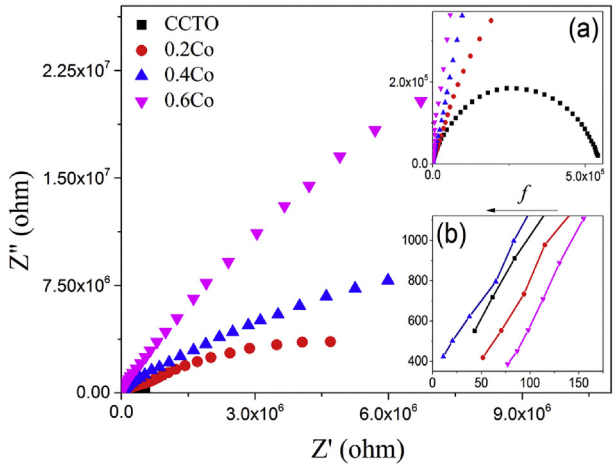

Fig. 6. The Cole-Cole plot of impedance for $CaCu_{3-x}Co_xTi_4O_{12}$ samples, at room temperature. The inset (a) illustrates the amplification of the overlapped region of these curves, and the inset (b) illustrates an enlarged view of the data close to the origin for the highest frequency.

$$tan\delta \approx 1/\omega R_{gb} C_P(\varepsilon) \quad (2)$$

where R_{gb} denotes the grain boundary resistance and can be determined at low frequencies by the extrapolated intercept of the arc on the Z' axis [47,48], while $C_p(\varepsilon)$ is the sample capacitance, which is proportional to the dielectric constant value (ε), related to Eq. (1). As seen in Fig. 6, at low frequencies, R_{gb} in Eq. (2) enhances with the increase in Co^{2+} concentration. The values of R_{gb} obtained for an undoped and the doped (x = 0.2, 0.4 and 0.6) samples are 5.5×10^5 Ω, 9.5×10^6 Ω, 3×10^7 Ω and 3.2×10^8 Ω, respectively (given in Table 1). The increase in the resistance by increasing Co^{2+} is mainly due to the decrease of the Cu-rich phase (CuO) and the formation of $CaTiO_3$ and Co_2TiO_4 phases at the grain boundaries, as mentioned earlier. According to Eq. (2), both R_{gb} and $C_p(\varepsilon)$ affect the value of the tanδ at low frequencies. Our results show that the undoped sample has the least value of R_{gb} and $C_p(\varepsilon)$ and thus, the tanδ is the highest compared to the doped samples, as can be seen in Fig. 5(b). However, the sample with x = 0.6 has the highest R_{gb} among all the samples, so it is expected that its tanδ decreases. Since, $C_p(\varepsilon)$ for this sample (x = 0.6) is smaller than that of the other two doped samples, according to Eq. (2), the tanδ is expected to increase. Nevertheless, since the tanδ for the sample with x = 0.6 is the smallest among all the other samples, we can conclude that in Eq. (2), R_{gb} is the dominant factor in reducing the dielectric loss in the doped samples at low frequencies, which is in agreement with other study [49]. Actually, at low frequencies, dc conductivity at the grain boundaries which is associated with R_{gb}, results in tanδ [50]. Our impedance spectroscopy analysis results confirm this explanation.

At high frequencies, the tanδ is approximately given as [15,43]:

$$\tan\delta \approx \omega R_g C_P(\varepsilon) \quad (3)$$

Table 1
The resistance of grains and grain boundaries of $CaCu_{(3-x)}Co_xTi_4O_{12}$ Ceramics [x = 0, 0.2, 0.4 and 0.6].

Sample	$R_g(\Omega)$	$R_{gb}(\Omega)$
$CaCu_3Co_0Ti_4O_{12}$	43	5.5×10^5
$CaCu_{2.8}Co_{0.2}Ti_4O_{12}$	52	9.5×10^6
$CaCu_{2.6}Co_{0.4}Ti_4O_{12}$	11	3×10^7
$CaCu_{2.4}Co_{0.6}Ti_4O_{12}$	77	3.2×10^8

where R_g denotes the semiconducting grain resistance, and can be estimated by nonzero intercept of the Z' axis which is shown in the inset of Fig. 6(b). The grain resistance of the all samples is found to be small in the range of 11–77 Ω, given in Table 1, which is agreement with others results [51,52]. As it can be seen in Fig. 5(a), changes in $C_p(\varepsilon)$ is remarkable compared to R_g at high frequencies. Therefore, in Eq. (3), $C_p(\varepsilon)$ is the dominant factor in increasing the tanδ in the doped samples, at high frequencies. As Fig. 5(a) shows the dielectric constant values of the doped samples are higher than that of the undoped sample, similar arguments can explain why the tanδ value is smaller for the undoped sample at high frequencies (Fig. 5(b)). So, it can be said that at high frequencies there is a reasonable correlation between the tanδ and the capacitance ($C_p(\varepsilon)$). It is also evident from Fig. 5(b) that at frequencies higher than 20 kHz, the tanδ increases with the increasing frequency for all samples, according to Eq. (3). However, it is obvious that at low frequencies (<1 kHz) the decrease of the tanδ is very significant. The values of the tanδ in the sample with x = 0.6 and the undoped sample at 50 Hz frequency are about 0.15 and 0.87, respectively. So, the dielectric loss has decreased about 8 times, at low frequencies. As mentioned before, the lower tanδ for the doped samples at low frequencies is due to the reduction in the Cu-rich phase (CuO) and the formation of CaTiO3 and Co_2TiO_4 phases at the grain boundaries (as shown in XRD patterns, SEM images and grain boundary EDX results), leading to the higher resistance at the boundaries. Since in our samples, the values of R_g are much less than R_{gb} as given in Table 1. Thus, according to IBLC model, this big difference between R_g and R_{gb} leads to a large polarization at the grain boundaries, causing the giant dielectric constant in CCTO [40]. The greater the difference is between R_{gb} and R_g, the stronger the interfacial polarization will be, leading to the increase in the dielectric constant [16]. Our results indicate that doping Co^{2+} into the CCTO ceramics enhances the resistance of the grain boundaries, and therefore, the dielectric constant of the doped samples becomes higher than that of the undoped sample.

The effect of the cobalt dopant concentration on the dielectric constant and tanδ at different frequencies for all the samples are given in Fig. 7(a and b), respectively. As can be seen in Fig. 7(a), the samples with x = 0.2 and x = 0.4 have larger dielectric constant values. Furthermore, the dielectric constant seems to become independent from cobalt dopant concentration, with the increase in the frequency. As Fig. 7(b) shows, the tanδ of the undoped sample is larger than that of the doped samples, at low and middle frequencies (50 Hz-1 kHz). However, at 10 kHz, the tanδ is almost independent of the cobalt concentration. The tanδ of the sample with x = 0.4 has a maximum value at higher frequencies. So, we can conclude that the concentration of cobalt dopant is an important factor considering the dielectric properties of the CCTO ceramics.

4. Conclusion

In this study, ceramics of $CaCu_{3-x}Co_xTi_4O_{12}$ (CCCTO, x = 0, 0.2, 0.4 and 0.6) were fabricated by a semi-wet route and the effects of substituting Cu^{2+} by Co^{2+} on the dielectric properties of the prepared samples were investigated. The samples were characterized using XRD, SEM and EDX techniques. The dielectric properties of the prepared samples were studied using a LCR meter, at different temperatures and frequencies. Our results showed that the dielectric constant of the samples increased with the increase in cobalt dopant concentration, while the dielectric loss decreased. These observations can be related to the reduction in the Cu-rich (CuO) phase and also the formation of $CaTiO_3$ and Co_2TiO_4 phases at the grain boundaries, which lead to the decrease in the grain boundaries conductivity. These results were confirmed by the XRD, SEM, EDX and also impedance spectroscopy (IS). Therefore, it can

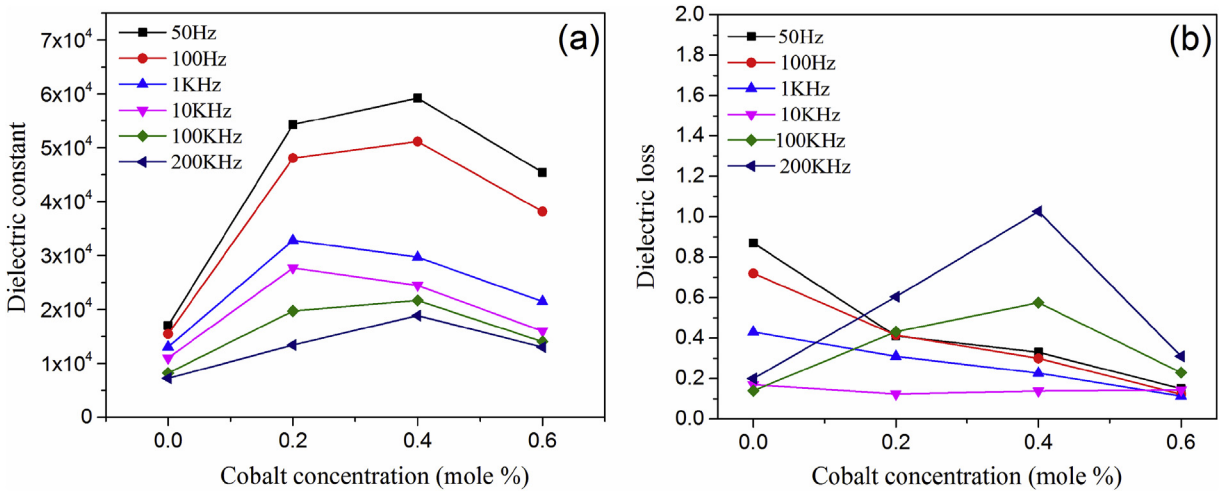

Fig. 7. The effect of cobalt dopant concentration on the (a) dielectric constant and (b) dielectric loss, at different frequencies.

be said that the substitution of Cu^{2+} by Co^{2+} in the CCTO ceramics enhances the dielectric constant in a broad range of frequencies and temperatures as well as decreasing the dielectric loss (tanδ) at low and middle frequencies, significantly. Regarding the application of CCCTO ceramics, we can conclude that for application in devices working in the temperature range of 300–600 K, the doped sample with x = 0.6 cobalt concentration seems to be the best composition. This sample shows the highest increase in the dielectric constant and also the highest decrease in the dielectric loss with increasing the temperature among the all prepared samples. Furthermore, for the devices working in a frequency range up to 20 kHz, particularly at urban power frequency, the sample with x = 0.4 cobalt concentration can be suggested to be the best composition, Because it shows the highest dielectric constant and also the lowest dielectric loss, in comparison with the other samples.

References

[1] J. Li, M. Subramanian, H. Rosenfeld, C. Jones, B. Toby, A. Sleight, Clues to the giant dielectric constant of CaCu3Ti4O12 in the defect structure of "SrCu3-Ti4O12", Chem. Mater. 16 (2004) 5223–5225.
[2] M. Subramanian, D. Li, N. Duan, B. Reisner, A. Sleight, High dielectric constant in ACu 3 Ti 4 O 12 and ACu 3 Ti 3 FeO 12 phases, J. Solid State Chem. 151 (2000) 323–325.
[3] C. Kant, T. Rudolf, F. Mayr, S. Krohns, P. Lunkenheimer, S. Ebbinghaus, A. Loidl, Broadband dielectric response of Ca Cu 3 Ti 4 O 12: from dc to the electronic transition regime, Phys. Rev. B 77 (2008) 045131.
[4] C. Homes, T. Vogt, S. Shapiro, S. Wakimoto, M. Subramanian, A. Ramirez, Charge transfer in the high dielectric constant materials CaCu 3 Ti 4 O 12 and CdCu 3 Ti 4 O 12, Phys. Rev. B 67 (2003) 092106.
[5] L. He, J. Neaton, M.H. Cohen, D. Vanderbilt, C. Homes, First-principles study of the structure and lattice dielectric response of CaCu 3 Ti 4 O 12, Phys. Rev. B 65 (2002) 214112.
[6] S.D. Hutagalung, L.Y. Ooi, Z.A. Ahmad, Improvement in dielectric properties of Zn-doped CaCu 3 Ti 4 O 12 electroceramics prepared by modified mechanical alloying technique, J. Alloys Compd. 476 (2009) 477–481.
[7] T.B. Adams, D.C. Sinclair, A.R. West, Giant barrier layer capacitance effects in CaCu 3 Ti 4 O 12 ceramics, Adv. Mater. 14 (2002) 1321–1323.
[8] T.T. Fang, H.K. Shiau, Mechanism for developing the boundary barrier layers of CaCu3Ti4O12, J. Am. Ceram. Soc. 87 (2004) 2072–2079.
[9] S. Jesurani, S. Kanagesan, K. Ashok, Microstructure and dielectrical responses of pure and cobalt-doped CaCu3Ti4O12 ceramics by sol–gel synthesis route, J. Sol-gel Sci. Technol. 64 (2012) 335–341.
[10] R. Mazumder, A. Seal, A. Sen, H.S. Maiti, Effect of boron addition on the dielectric properties of giant dielectric CaCu3Ti4O12, Ferroelectrics 326 (2005) 103–108.
[11] A.E. Smith, T. Calvarese, A. Sleight, M. Subramanian, An anion substitution route to low loss colossal dielectric CaCu 3 Ti 4 O 12, J. Solid State Chem. 182 (2009) 409–411.
[12] E. Paisley, M. Losego, S. Aygun, H. Craft, J.-P. Maria, Barrier layer mechanism engineering in calcium copper titanate thin film capacitors through micro-structure control, J. Appl. Phys. 104 (2008) 114110.
[13] C.-H. Mu, P. Liu, Y. He, J.-P. Zhou, H.-W. Zhang, An effective method to decrease dielectric loss of CaCu 3 Ti 4 O 12 ceramics, J. Alloys Compd. 471 (2009) 137–141.
[14] S. Jin, H. Xia, Y. Zhang, Effect of La-doping on the properties of CaCu 3 Ti 4 O 12 dielectric ceramics, Ceram. Int. 35 (2009) 309–313.
[15] Y. Yan, L. Jin, L. Feng, G. Cao, Decrease of dielectric loss in giant dielectric constant CaCu 3 Ti 4 O 12 ceramics by adding CaTiO 3, Mater. Sci. Eng. B 130 (2006) 146–150.
[16] C. Mu, H. Zhang, Y. He, P. Liu, Influence of temperature on dielectric properties of Fe-doped CaCu 3 Ti 4 O 12 ceramics, Phys. B Condens. Mat. 405 (2010) 386–389.
[17] L. Xu, P. Qi, X. Song, X. Luo, C. Yang, Dielectric relaxation behaviors of pure and Pr 6 O 11-doped CaCu 3 Ti 4 O 12 ceramics in high temperature range, J. Alloys Compd. 509 (2011) 7697–7701.
[18] R. Xue, Z. Chen, H. Dai, D. Liu, T. Li, G. Zhao, Effects of rare earth ionic doping on microstructures and electrical properties of CaCu 3 Ti 4 O 12 ceramics, Mater. Res. Bull. 66 (2015) 254–261.
[19] H.A. Ardakani, M. Alizadeh, R. Amini, M.R. Ghazanfari, Dielectric properties of CaCu 3 Ti 4 O 12 improved by chromium/lanthanum co-doping, Ceram. Int. 38 (2012) 4217–4220.
[20] S. Jesurani, S. Kanagesan, M. Hashim, I. Ismail, Dielectric properties of Zr doped CaCu 3 Ti 4 O 12 synthesized by sol–gel route, J. Alloys Compd. 551 (2013) 456–462.
[21] D. Xu, K. He, R. Yu, X. Sun, Y. Yang, H. Xu, H. Yuan, J. Ma, High dielectric permittivity and low dielectric loss in sol–gel derived Zn doped CaCu 3 Ti 4 O 12 thin films, Mater. Chem. Phys. 153 (2015) 229–235.
[22] C.K. Yeoh, M.F. Ahmad, Z.A. Ahmad, Effects of Cu and Ti excess on the dielectric properties of CaCu 3 Ti 4 O 12 prepared using a wet chemical method, J. Alloys Compd. 443 (2007) 155–160.
[23] A. Rahnama, M. Gharagozlou, Preparation and properties of semiconductor CuO nanoparticles via a simple precipitation method at different reaction temperatures, Opt. Quantum Electron. 44 (2012) 313–322.
[24] E. Cockayne, B.P. Burton, Phonons and static dielectric constant in CaTiO 3 from first principles, Phys. Rev. B 62 (2000) 3735.
[25] A. Krause, Ultrathin CaTiO3 Capacitors: Physics and Application, 2013.
[26] M. Prosnikov, A. Molchanova, R. Dubrovin, K. Boldyrev, A. Smirnov, V.Y. Davydov, A. Balbashov, M. Popova, R. Pisarev, Lattice dynamics and electronic structure of cobalt–titanium spinel Co2TiO4, Phys. Solid State 58 (2016) 2516–2522.
[27] A.K. Rai, K. Mandal, D. Kumar, O. Parkash, Characterization of nickel doped CCTO: CaCu 2.9 Ni 0.1 Ti 4 O 12 and CaCu 3 Ti 3.9 Ni 0.1 O 12 synthesized by semi-wet route, J. Alloys Compd. 491 (2010) 507–512.
[28] J.J. Mohamed, S.D. Hutagalung, M.F. Ain, K. Deraman, Z.A. Ahmad, Micro-structure and dielectric properties of CaCu 3 Ti 4 O 12 ceramic, Mater. Lett. 61 (2007) 1835–1838.
[29] C.-L. Huang, M.-H. Weng, C.-C. Yu, Low firable BiNbO 4 based microwave dielectric ceramics, Ceram. Int. 27 (2001) 343–350.
[30] T. Gladman, On the theory of the effect of precipitate particles on grain growth in metals, Proc. R. Soc. Lond. A Math. Phys. Eng. Sci. R. Soc. (1966) 298–309.
[31] W. Kingery, H. Bowen, D. Uhlmann, Introduction to Ceramics, Jhon Willey & Sons, New York, 1976.
[32] R. Abbaschian, R.E. Reed-Hill, Physical Metallurgy Principles, Cengage Learning, 2008.
[33] Z. Jeffries, R.S. Archer, The Science of Metals, McGraw-Hill, 1924.
[34] B. Bender, M.-J. Pan, The effect of processing on the giant dielectric properties

of CaCu 3 Ti 4 O 12, Mater. Sci. Eng. B 117 (2005) 339–347.
[35] S. Shao, J. Zhang, P. Zheng, W. Zhong, C. Wang, Microstructure and electrical properties of Ca Cu 3 Ti 4 O 12 ceramics, J. Appl. Phys. 99 (2006) 084106.
[36] L. Ni, X.M. Chen, Dielectric relaxations and formation mechanism of giant dielectric constant step in CaCu3Ti4O12 ceramics, Appl. Phys. Lett. 91 (2007) 122905.
[37] C. Wang, L. Zhang, Surface-layer effect in CaCu3Ti4O12, Appl. Phys. Lett. 88 (2006) 2906.
[38] S. Sahoo, U. Dash, S. Parashar, S. Ali, Frequency and temperature dependent electrical characteristics of CaTiO3 nano-ceramic prepared by high-energy ball milling, J. Adv. Ceram. 2 (2013) 291–300.
[39] K. Mandal, A.K. Rai, L. Singh, O. Parkash, Dielectric properties of CaCu 2· 9 Co 0· 1 Ti 4 O 12 and CaCu 3 Ti 3· 9 Co 0· 1 O 12 ceramics synthesized by semi-wet route, Bull. Mater. Sci. 35 (2012) 433–438.
[40] Z. Yang, Y. Zhang, G. You, K. Zhang, R. Xiong, J. Shi, Dielectric and electrical transport properties of the Fe 3+-doped CaCu 3 Ti 4 O 12, J. Mater. Sci. Technol. 28 (2012) 1145–1150.
[41] C. Homes, T. Vogt, S. Shapiro, S. Wakimoto, A. Ramirez, Optical response of high-dielectric-constant perovskite-related oxide, Science 293 (2001) 673–676.
[42] F. Amaral, M. Valente, L. Costa, Dielectric properties of CaCu 3 Ti 4 O 12 (CCTO) doped with GeO 2, J. Non-Cryst. Solids 356 (2010) 822–827.
[43] T. Li, J. Chen, D. Liu, Z. Zhang, Z. Chen, Z. Li, X. Cao, B. Wang, Effect of NiO-doping on the microstructure and the dielectric properties of CaCu 3 Ti 4 O 12 ceramics, Ceram. Int. 40 (2014) 9061–9067.
[44] W. Ni, X. Zheng, J. Yu, Sintering effects on structure and dielectric properties of dielectrics CaCu 3 Ti 4 O 12, J. Mater. Sci. 42 (2007) 1037–1041.
[45] J.T. Irvine, D.C. Sinclair, A.R. West, Electroceramics: characterization by impedance spectroscopy, Adv. Mater. 2 (1990) 132–138.
[46] V. Brizé, G. Gruener, J. Wolfman, K. Fatyeyeva, M. Tabellout, M. Gervais, F. Gervais, Grain size effects on the dielectric constant of CaCu 3 Ti 4 O 12 ceramics, Mater. Sci. Eng. B 129 (2006) 135–138.
[47] K.S. Cole, R.H. Cole, Dispersion and absorption in dielectrics I. Alternating current characteristics, J. Chem. Phys. 9 (1941) 341–351.
[48] K.S. Cole, R.H. Cole, Dispersion and absorption in dielectrics II. Direct current characteristics, J. Chem. Phys. 10 (1942) 98–105.
[49] J. He, F. Luo, J. Hu, Y. Lin, Cu segregation and its effects on the electrical properties of calcium copper titanate, Sci. China Technol. Sci. 54 (2011) 2506–2510.
[50] A. Thomas, K. Abraham, J. Thomas, K. Saban, Structural and dielectric properties of A-and B-sites doped CaCu 3 Ti 4 O 12 ceramics, Ceram. Int. 41 (2015) 10250–10255.
[51] Q. Zheng, H. Fan, C. Long, Microstructures and electrical responses of pure and chromium-doped CaCu 3 Ti 4 O 12 ceramics, J. Alloys Compd. 511 (2012) 90–94.
[52] L. Feng, X. Tang, Y. Yan, X. Chen, Z. Jiao, G. Cao, Decrease of dielectric loss in CaCu3Ti4O12 ceramics by La doping, Phys. Status Solidi (a) 203 (2006) R22–R24.